

## **Supplementary information**

### **Human adipose tissue-derived mesenchymal stem cells secrete functional neprilysin-bound exosomes**

Takeshi Katsuda, Reiko Tsuchiya, Nobuyoshi Kosaka, Yusuke Yoshioka, Kentaro Takagaki, Katsuyuki Oki, Fumitaka Takeshita, Yasuyuki Sakai, Masahiko Kuroda, and Takahiro Ochiya

#### **Supplementary Table 1. Donor information for used adipose tissue-derived mesenchymal stem cells.**

#### **Supplementary Table 2. Donor information for used bone marrow-derived mesenchymal stem cells.**

## **Supplementary figure legends**

### **Fig. S1. Surface marker profiles of ADSCs and BM-MSCs.**

Both cells showed similar surface marker profiles that are characteristic of MSCs (positive for CD105, CD73, CD90, and CD44; negative for CD45, CD31, and CD34).

### **Fig. S2. NEP enzyme activity of ADSC lysates.**

Enzyme activity was measured using a fluorogenic substrate for ADSCs #1–3 (A, B) and ADSCs #4–6 (C, D) in the absence or presence of the NEP inhibitor thiorphan. Data are the mean  $\pm$  S.D. ( $n = 3$ ). In each experiment, the enzyme activity rate was determined as the gradient of the fluorescence intensity versus time plots in the linear region (where  $R^2 > 0.97$ ). Enzyme activity was also measured for rhNEP dilution series to produce a standard curve (E, G). Good standard curves were obtained in each experiment ( $R^2 > 0.99$ ) (F, H) and were used to determine the NEP activity indices.

### **Fig. S3. NEP enzyme activity of BM-MSC lysates.**

Enzyme activity was measured using a fluorogenic substrate for BM-MSCs #1-4 and ADSC #4 for comparison in the absence (A) or presence (B) of the NEP inhibitor thiorphan. The specific NEP activity was calculated by subtracting residual fluorescent intensity after incubation with the NEP inhibitor thiorphan. Data are the mean  $\pm$  S.D. ( $n = 3$ ).

### **Fig. S4. Calculation of NEP activity index of ADSC-derived exosomes.**

Enzyme activity was measured using a fluorogenic substrate for exosomes from ADSCs

#1–4 in the presence and absence of the NEP inhibitor thiorphan (Fig 4B-D). In each experiment, the enzyme activity rate was determined as the gradient of the fluorescence intensity versus time plots in the linear region (where  $R^2 > 0.97$ ). Enzyme activity was also measured for rhNEP dilution series (A) to produce a standard curve (B). ( $R^2 > 0.99$ ). Using the produced standard curve, NEP activity indices was calculated (Fig. 4F).

**Fig. S5. Effect of ADSC-derived exosomes on the intracellular A $\beta$ 42 level of N2a cells.**

(a) The schematic representation of the experiment. (b) ADSC-derived exosomes decrease slightly, but significantly, the intracellular A $\beta$ 42 level in the recipient N2a cells. Data are the mean  $\pm$  S.D. (n = 4).

**Fig. S6. NEP contribution ratio for BM-MSD-derived exosomes**

Shown are the NEP contribution ratios for exosomes derived from BM-MSDs #1 and #4 (right 2 columns) in comparison with that for ADSC #2-derived exosomes (left column). Data are the mean  $\pm$  S.D. (n = 3).

**Table S1. Donor information for used adipose tissue-derived mesenchymal stem cells.**

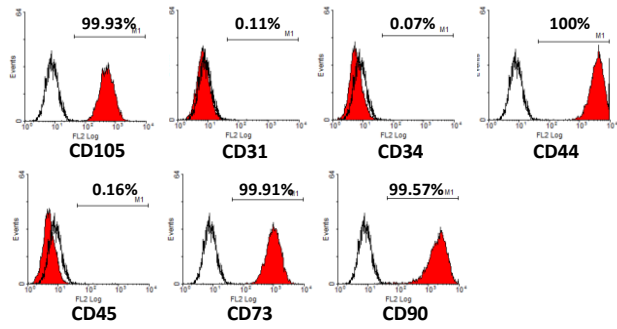
<b>ID</b>	#1	#2	#3	#4	#5	#6
<b>Sex</b>	Female	Female	Female	Female	Female	Female
<b>Age</b>	42	22	45	22	49	23
<b>Site</b>	Flanks, Hips, Thighs (Subcutaneous)	Flanks, Hips, Thighs (Subcutaneous)	Flanks, Hips, Thighs (Subcutaneous)	Abdomen, Flanks (Subcutaneous)	Abdomen, Flanks (Subcutaneous)	Hips, Thighs (Subcutaneous)

**Table S2. Donor information for used bone marrow-derived mesenchymal stem cells.**

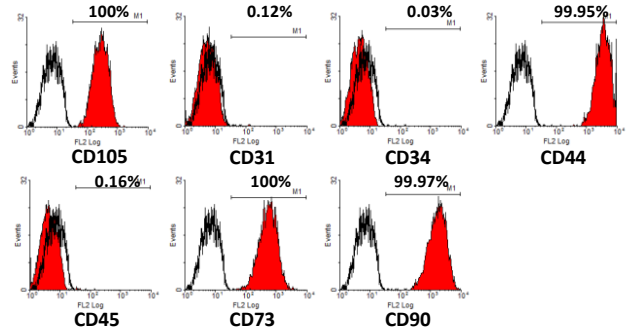
<b>ID</b>	#1	#2	#3	#4
<b>Sex</b>	Male	Male	Male	Male
<b>Age</b>	55	30	64	21
<b>Site</b>	Ilium	Ilium	Ilium	No information

# Fig. S1

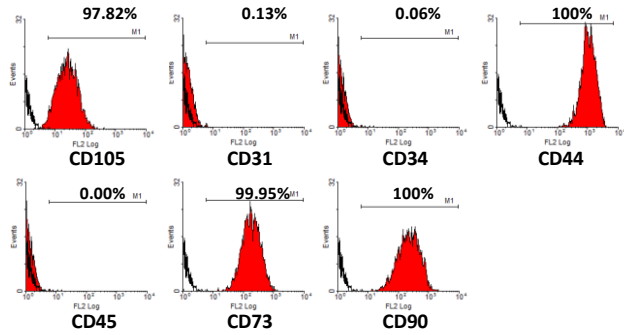
## BM-MSC #1



## BM-MSC #4



## ADSC #1



## ADSC #4

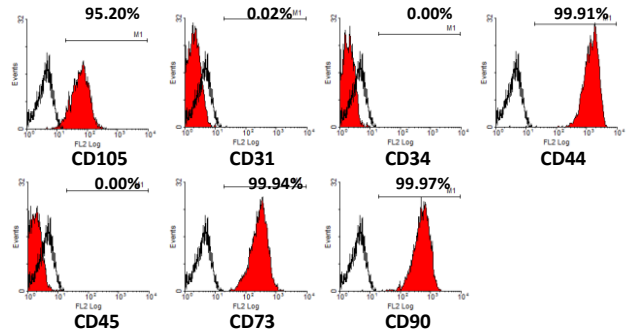
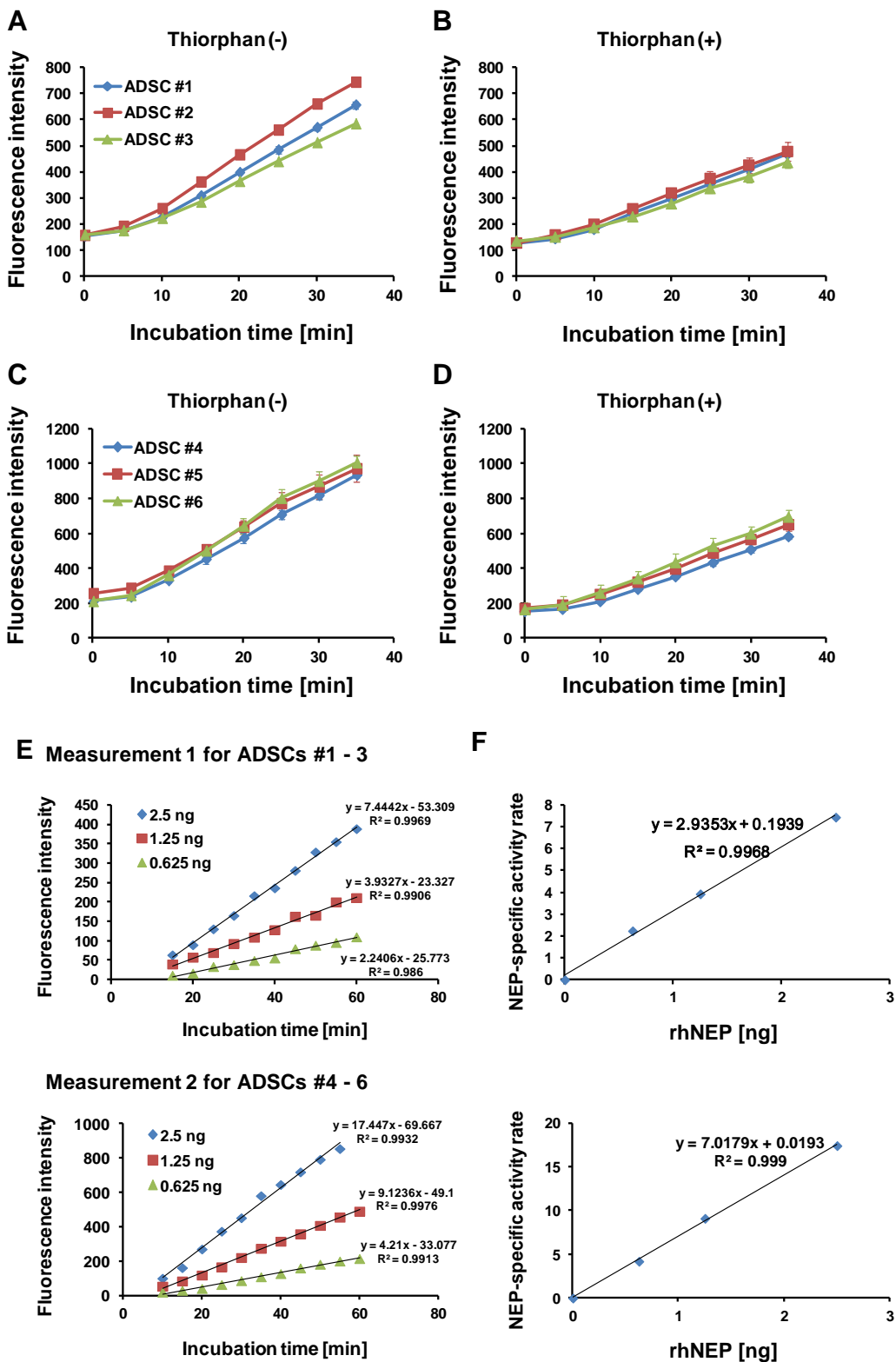
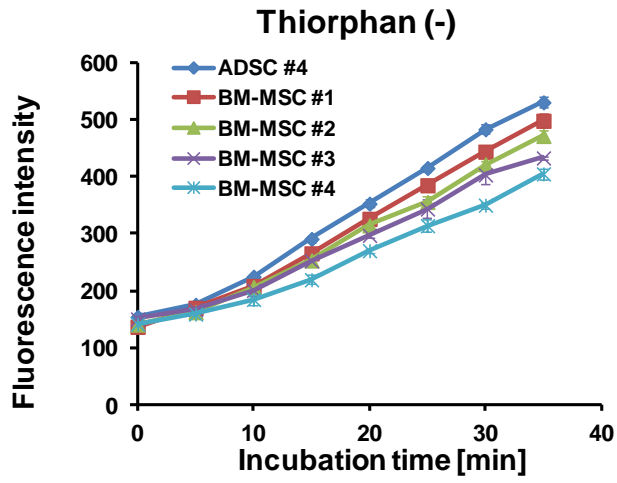


Fig. S2



**Fig. S3**

**A**



**B**

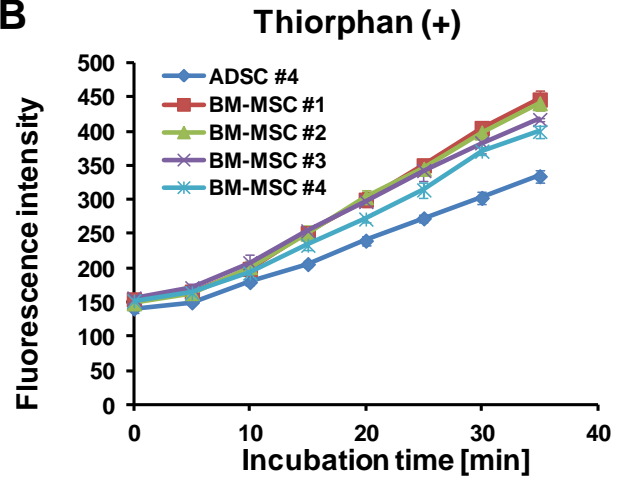


**Fig. S4**

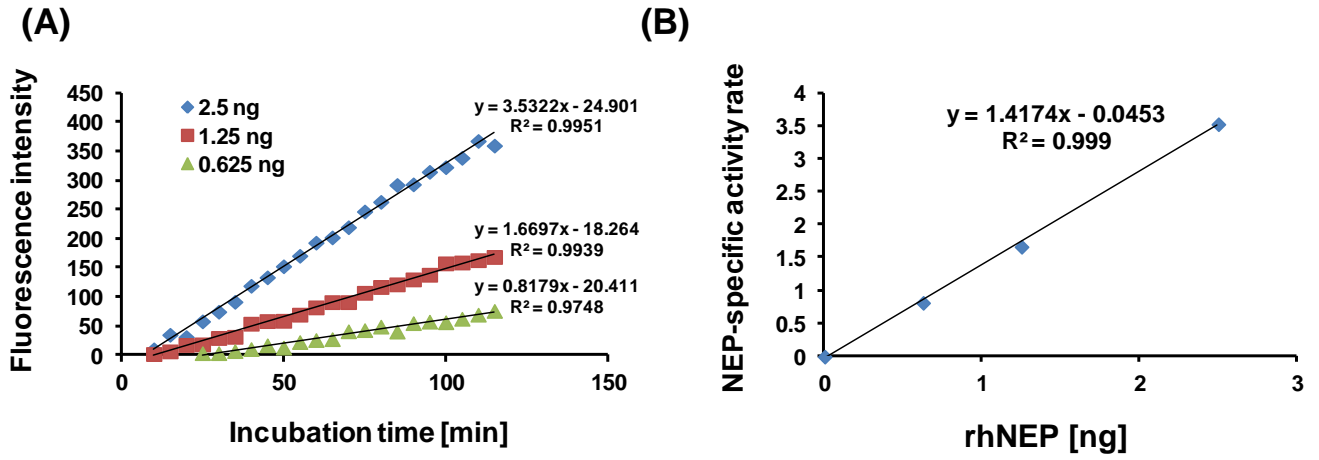
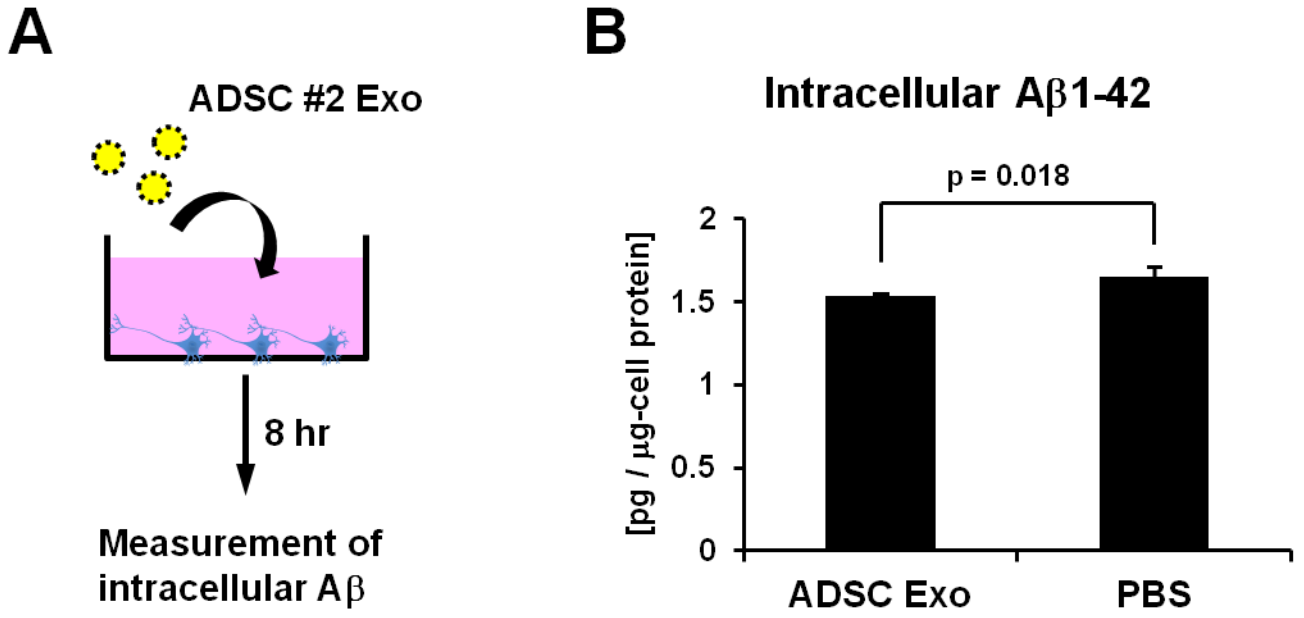




Fig. S5



**Fig. S6**

